Nationaal Lucht- en Ruimtevaartlaboratorium
National Aerospace Laboratory NLR

Executive summary

Small-Scale Helicopter Blade Flap-Lag Equations of Motion For A Flybarless Pitch-Lag-Flap Main Rotor

Problem area
We derive the coupled flap-lag equations of motion, for a small-scale helicopter flybarless rotor, in the case of a rigid articulated Pitch-Lag-Flap (P-L-F) hinges arrangement.

Description of work
The derivation allows for hinge springs and viscous dampers, for both Clock-Wise (CW) and Counter-ClockWise (CCW) rotating main rotors, while keeping all hinges physically separated. The equations are obtained by the Lagrangian method, which requires only velocity and position terms, and is much more convenient for overall system modeling. Further the flap-lag dynamics are valid for small flap, lag, and pitch angles. As the exact tangential and perpendicular blade velocity expressions have been retained, full coupling between vehicle and blade dynamics is modeled. Additionally the paper reviews all assumptions made in deriving the model, i.e. structural, aerodynamics, and dynamical simplifications.

Results and conclusions
The model has been compared with an equivalent FLIGHTLAB rotor model, in hover and at high speed. The amplitude and frequency match for the flap, lag, and TPP angles is good to very good for both test conditions, while the amplitude and frequency match of flap and lag velocities is good in hover and fair at high speed.

Applicability
First the (P-L-F) sequence is a useful arrangement for modeling the rotor dynamics of R/C helicopters. Further the present blade flap-lag model could potentially be integrated into a small-scale helicopter flight dynamics model for the purpose of high bandwidth control synthesis.

Report no.
NLR-TP-2011-229

Author(s)
S. Taamallah

Report classification
UNCLASSIFIED

Date
July 2011

Knowledge area(s)
Helikoptertechnologie

Descriptor(s)
Unmanned Aerial Vehicle (UAV)
Main rotor flap-lag

This report is based on a presentation held at the AIAA Modeling and Simulation Technologies Conference, Portland, Oregon, USA, 8 - 11 August 2011.

Small-Scale Helicopter Blade Flap-Lag Equations of Motion For A Flybarless Pitch-Lag-Flap Main Rotor

Nationaal Lucht- en Ruimtevaartlaboratorium, National Aerospace Laboratory NLR

Anthony Fokkerweg 2, 1059 CM Amsterdam,
P.O. Box 90502, 1006 BM Amsterdam, The Netherlands
Telephone +31 20 511 31 13, Fax +31 20 511 32 10, Web site: www.nlr.nl

Nationaal Lucht- en Ruimtevaartlaboratorium
National Aerospace Laboratory NLR

NLR-TP-2011-229

Small-Scale Helicopter Blade Flap-Lag Equations of Motion For A Flybarless Pitch-Lag-Flap Main Rotor

S. Taamallah

This report is based on a presentation held at the AIAA Modeling and Simulation Technologies Conference, Portland, Oregon, USA, 8 - 11 August 2011.

Customer	National Aerospace Laboratory NLR
Contract number	----
Owner	National Aerospace Laboratory NLR
Division NLR	Aerospace Systems and Applications
Distribution	Unlimited
Classification of title	Unclassified
	July 2011

Approved by:

Author	Reviewer	Managing department
	19/8/2011	19/08/2011

Contents

This page is intentionally left blank.

Small-Scale Helicopter Blade Flap-Lag Equations of Motion for a Flybarless Pitch-Lag-Flap Main Rotor

Skander Taamallah*†

National Aerospace Laboratory (NLR), 1059CM Amsterdam, The Netherlands

We derive the coupled flap-lag equations of motion, for a small-scale helicopter flybarless rotor, in the case of a rigid articulated Pitch-Lag-Flap (P-L-F) hinge arrangement. The (P-L-F) sequence is indeed much more useful for modeling the rotor dynamics of R/C helicopters. The derivation, obtained by the Lagrangian method, allows for hinge springs and viscous dampers, for both ClockWise (CW) and Counter-ClockWise (CCW) rotating main rotors, while keeping all hinges physically separated. Although the equations are valid for small flap, lag, and pitch angles, the exact tangential and perpendicular blade velocity expressions have been retained, hence full coupling between vehicle and blade dynamics is modeled. Additionally the paper reviews all assumptions made in deriving the model, i.e. structural, aerodynamics, and dynamical simplifications. The model has been compared with an equivalent FLIGHTLAB® rotor model, and simulation results show that the model validity is good to very good in hover and low speed, and fair to good at high speed.

Nomenclature

Vectors in this paper are printed in boldface $\mathbf{X}$ and are defined in $\mathbb{R}^3$. A vector is qualified by its subscript while its superscript denotes the projection frame. Matrices are written in outline type $\mathbb{M}$. All frames are 3-D orthogonal and right-handed. Transformation matrices are denoted as $\mathbb{T}_{ij}$, with the two suffices signifying from frame F_j to frame F_i. For the kinematics frames, we adopt here the notation used in Ref. 1, for blade frames see figure 1 and figure 2.

Frames

F_I	Geocentric inertial frame
F_E	Normal earth fixed frame
F_o	Vehicle carried normal earth frame
F_b	Body (vehicle) frame
F_a	Aerodynamic (air path) frame
F_k	Kinematic (flight path) frame
F_{HB}	Hub-Body frame

Kinematics

ψ	Azimuth angle (yaw angle, heading)
θ	Inclination angle (pitch angle, or elevation)
ϕ	Bank angle (roll angle)
$\mathbf{V}_{k,G}$	Kinematic velocity of the vehicle center of mass
$\mathbf{V}_{a,G}$	Aerodynamic velocity of the vehicle center of mass
$\mathbf{V}_w$	Wind linear velocity in F_o, of an atmospheric particle which could have been located at the vehicle center of mass

*R&D Engineer, Avionics Systems Department, National Aerospace Laboratory (NLR), 1059CM Amsterdam, The Netherlands.

†Ph.D. Student, Delft Center for Systems and Control (DCSC), Faculty of Mechanical, Maritime and Materials Engineering, Delft University of Technology, 2628CD Delft, The Netherlands.

$u_k^o = V_N$	x component of $\mathbf{V}_{k,G}$ on F_o, V_N North velocity
$v_k^o = V_E$	y component of $\mathbf{V}_{k,G}$ on F_o, V_E East velocity
$w_k^o = V_Z$	z component of $\mathbf{V}_{k,G}$ on F_o, V_Z Vertical velocity
$u_k^b = u$	x component of $\mathbf{V}_{k,G}$ on body frame F_b
$v_k^b = v$	y component of $\mathbf{V}_{k,G}$ on body frame F_b
$w_k^b = w$	z component of $\mathbf{V}_{k,G}$ on body frame F_b
u_w	Wind x-velocity in F_o
v_w	Wind y-velocity in F_o
w_w	Wind z-velocity in F_o
$\mathbf{\Omega}_k = \mathbf{\Omega}_{bo}$	Kinematic angular velocity of the vehicle relative to the earth
$p_k^b = p$	Roll velocity (roll rate) of the vehicle relative to the earth
$q_k^b = q$	Pitch velocity (pitch rate) of the vehicle relative to the earth
$r_k^b = r$	Yaw velocity (yaw rate) of the vehicle relative to the earth
a	Speed of sound
g	Gravity constant
M	Mach number
ρ	Air density

Main rotor and main rotor blade

B	Tip loss factor, expressed as percentage of blade length R_{bl}
c_{bl}	Blade chord
$c_{d_{bl}}$	Blade section drag coefficient
c_{hub}	Hub arm chord
$c_{l_{bl}}$	Blade section lift coefficient
I_β	Blade 2nd mass moment (inertia about flap hinge)
K_{D_β}	Hub spring damping coefficient (due to flap)
K_{D_ζ}	Hub spring damping coefficient (due to lag)
K_{S_β}	Hub spring restraint coefficient (due to flap)
K_{S_ζ}	Hub spring restraint coefficient (due to lag)
$K_{(\theta\beta)}$	Pitch-flap coupling ratio
$K_{(\theta\zeta)}$	Pitch-lag coupling ratio
M_{bl}	Blade 0th mass moment (blade mass from flap hinge)
N_b	Main rotor number of blades
r_{dm}	Distance between flap hinge and blade element dm
R_{bl}	Blade radius measured from flap hinge
R_{rot}	Rotor radius measured from hub center
U_P	Flow velocity perpendicular to the reference $(x_{F_{ref}}, y_{F_{ref}})$ plane
U_T	Flow velocity tangential to the reference $(x_{F_{ref}}, y_{F_{ref}})$ plane
v_i	Rotor induced velocity
x_H, y_H, z_H	Position of main rotor Hub center wrt vehicle Center of Gravity (CG)
$x_{G_{bl}}, y_{G_{bl}}, z_{G_{bl}}$	Position of blade CG wrt flap hinge
α_{bl}	Blade section angle of attack
β_P	Rotor precone angle
β_{bl}	Blade flap angle
β_0	Rotor Tip-Path-Plane (TPP) coning angle
β_{1c}	Longitudinal rotor TPP tilt (positive forward)
β_{1s}	Lateral rotor TPP tilt (positive towards retreating side)
Γ	Direction of rotation, $CCW : \Gamma = 1 \quad CW : \Gamma = -1$
$\Omega_{MR_{100\%}}$	Nominal (100%) main rotor angular velocity
Ω_{MR}	Instantaneous main rotor angular velocity
ψ_{bl}	Azimuthal angular position of blade
ψ_{PA}	Swashplate phase angle
θ_{bl}	Blade pitch outboard of flap hinge (feathering) angle
θ_0	Blade root collective pitch
θ_{1c}	Lateral cyclic pitch

θ_{1s}	Longitudinal cyclic pitch
ζ_{bl}	Blade lag angle

I. Introduction

The main rotor is the single most important helicopter module of any component-type mathematical model.[2] In a fully articulated rotor system, each rotor blade is attached to the rotor hub through a series of hinges, which allow the blade to move independently of the others. Hence the blades are allowed to feather (pitch), flap, and lead-lag independently of each other.[3] For a single main rotor, and briefly summarized, helicopter flight dynamics includes the rigid-body responses combined with higher-frequency modes.[4] These higher-frequency modes are generated by the main rotor system, and its interaction with the fuselage and other vehicle components. For flight mechanics and control development purposes, the three most important aspects of these higher order rotor dynamics are blade flapping which allows the blade to move in a plane containing the blade and the shaft, blade lead-lag which allows the blade to move in the plane of rotation, and rotor inflow which is the flow field induced by the rotor at the rotor disk.

I.A. Background

Already since the early 1950s it had been known that including flapping dynamics in a helicopter flight model could produce limitations in rate and attitude feedback gains.[5] In fact blade flapping motion has three natural modes, i.e. coning, advancing, and regressing. The regressing flapping mode is the most relevant when considering the effect of rotor dynamics on handling characteristics, it is the lowest frequency mode of the three, and it has a tendency to couple into the fuselage modes.[6–12] Additionally for helicopter directional axis control, blade lead-lag dynamics ought to be considered for control system design.[13] In particular it is well known that blade lead-lag produces increased phase lag at high frequency, in the same frequency range where flapping effects occur,[10] and that control rate gains are primarily limited by lead-lag-body coupling.[10,14]

I.B. Small-Scale Helicopter Main Rotor

In the case of a small-scale helicopter, the rotor hub generally includes a feathering hinge close to the shaft, and a lead-lag hinge[a] a little further away. Besides the hub is typically not equipped with a flap hinge, this latter is often replaced by stiff rubber rings, hence a so-called hingeless flap mechanism. But for the purpose of modeling it is standard practice in helicopter theory to model a hingeless rotor (and its flexible blades) as a rotor having rigid blades with the blades attached to a virtual flap hinge,[15] this latter being offset from the main rotor axis. This virtual hinge is often modeled as a torsional spring, implying stiffness and damping. It is therefore by adjusting the virtual hinge offset distance, stiffness and damping that we can recreate the correct blade flap motion, in terms of amplitude and frequency.[16,17] Now for the purpose of modeling a generic small-scale helicopter flybarless[b] rotor, we have chosen to select an articulated Pitch-Lag-Flap (P-L-F) hinge arrangement, placing the virtual flap hinge outboard of the lag hinge, see figure 1 and figure 2. This configuration allows for unrestricted flap hinge displacement outboard of the lag hinge, while keeping the option of having the pitch and lag hinge offsets at their current physical values.

I.C. Our Blade Flap-Lag Model

In terms of blade flap-lag modeling a foundational contribution was given in Ref. 18, where derivations of the coupled flap-lag equations of motion for a rigid articulated rotor with hinge springs and viscous dampers, for the (F-L-P), (F-P-L), and (L-F-P) sequences were laid out. The purpose of our work is to present the rigid blade coupled flap-lag equations of motion for a new hinge arrangement, i.e. the (P-L-F) sequence, which is much more useful for modeling the rotor dynamics of small-scale flybarless R/C helicopters. The equations, obtained by the Lagrangian method,[19] are valid for a single articulated[c] rotor, with hinge springs and viscous dampers. Compared to Ref. 18 our approach retains all three hinges physically separated and

[a] Which is technically not a hinge, we refer here to the blade fixation bolt.

[b] Flybarless, i.e. without a Bell-Hiller stabilizing bar.

[c] Although this model with a proper combination of hinge offset and springs about the hinge could also be used to model a hingeless rotor.

works also for both CW and CCW rotating main rotors. Although the flap-lag equations of motion are valid for small flap - lag - pitch angles, the exact tangential and perpendicular blade velocity expressions have been retained, hence full coupling between vehicle and blade dynamics is modeled. Additionally, computation of main rotor forces was done numerically, through Gaussian quadrature integration, using a low order Legendre polynomial scheme.[20,21] The paper reviews all assumptions made in deriving the model, i.e. structural, aerodynamics, and dynamical simplifications, which are valid for stability and control investigations of helicopters up to an advance ratio limit[d] of about 0.3.[8,22,23]

The remainder of the paper is organized as follows. In Section II, the modeling assumptions are reviewed. In Sections III, the inertial position and velocity of a blade element are presented. In Section IV, the flap-lag equations of motion are derived. In Section V, simulation results are discussed. Finally, conclusions and future directions are presented in Section VI.

II. Modeling Assumptions

Structural Simplifications

- Rotor shaft forward and lateral tilt-angles are zero. Blade has zero twist, constant chord, zero sweep, constant thickness ratio, and a uniform mass distribution.
- Rigid rotor blade in bending. Neglecting higher modes (harmonics), since higher modes are only pronounced at high speed.[15,24] Further blade torsion is neglected, since small-scale helicopter blades are generally relatively stiff.
- Rotor inertia inboard of the flap hinge is assumed small and thus neglected.

Aerodynamics Simplifications

- Vehicle flies at a low altitude, hence neglecting air density and temperature variations. Blade element theory[e] is used to compute rotor lift and drag forces. Radial flow along blade span is ignored. Pitch, lag, and flap angles are assumed to be small.
- Compressibility effects are disregarded, which is a reasonable assumption considering small-scale helicopter flight characteristics. Viscous flow effects are also disregarded, which is a valid assumption for low angle of attacks and unseparated flow.[25,26]
- Forces inboard of the flap hinge are assumed small and thus neglected.

Dynamical Simplifications

- Dynamic twist[f] is neglected. Hence blade CG is assumed to be located on the blade section quarter chord line.
- Unsteady (frequency dependent) effect for time-dependent development of blade lift and pitching moment, due to changes in local incidence are ignored. For example dynamic stall, due to rapid pitch changes, is ignored.

III. Position and Velocity of a Blade Element

In the Hub-Body frame F_{HB}, see figure 1 and figure 2, the position of a blade element dm is given by

$$\begin{pmatrix} x_{dm} \\ y_{dm} \\ z_{dm} \end{pmatrix}^{HB} = \mathbb{T}_{(HB)6} \left\{ \mathbb{T}_{54} \left[\mathbb{T}_{32} \left(\mathbb{T}_{1(bl)} \begin{pmatrix} 0 \\ r_{dm} \\ 0 \end{pmatrix} + \begin{pmatrix} 0 \\ e_F \\ 0 \end{pmatrix} \right) + \begin{pmatrix} 0 \\ e_L \\ 0 \end{pmatrix} \right] + \begin{pmatrix} 0 \\ e_P \\ 0 \end{pmatrix} \right\} \quad (1)$$

[d] The flight envelope of small-scale helicopters is well within this limit.

[e] Calculates the forces on the blade due to its motion through the air. It is assumed that each blade section acts as a 2-D airfoil to produce aerodynamic forces, with the influence of the wake contained in an induced angle of attack at the blade section.[3]

[f] Any offset in blade chordwise CG or aerodynamic center position will result in a coupling of the flap and torsion Degrees Of Freedom (DOF) in blade elastic modes.[15]

And the inertial position of a blade element dm is given by

$$\mathbf{AP_{dm}} = \mathbf{AG} + \mathbf{GH} + \mathbf{HP_{dm}} = \mathbf{AG} + \begin{pmatrix} x_H \\ y_H \\ z_H \end{pmatrix} + \begin{pmatrix} x_{dm} \\ y_{dm} \\ z_{dm} \end{pmatrix} \tag{2}$$

The inertial velocity of a blade element dm positioned at P_{dm}, is defined as $\mathbf{V}_{I,P_{dm}}$ relative to the inertial frame F_I. Projecting in the Hub-Body frame F_{HB} we obtain

$$\mathbf{V}^{HB}_{I,P_{dm}} = \left(\frac{d\mathbf{AG}^I}{dt}\right)^{HB} + \left(\frac{d\mathbf{GH}^I}{dt}\right)^{HB} + \left(\frac{d\mathbf{HP_{dm}}^I}{dt}\right)^{HB} \tag{3}$$

For the first term on the Right-Hand-Side (RHS) of Eq (3), and assuming a flat and fixed earth we get

$$\left(\frac{d\mathbf{AG}^I}{dt}\right)^{HB} = \mathbb{T}_{(HB)o}\mathbf{V}^o_{k,G} = \mathbb{T}_{(HB)o}\begin{pmatrix} V_N \\ V_E \\ V_Z \end{pmatrix}^o \tag{4}$$

For the second term on the RHS of Eq (3) we have

$$\left(\frac{d\mathbf{GH}^I}{dt}\right)^{HB} = \left(\frac{d\mathbf{GH}^b}{dt}\right)^{HB} + \mathbf{\Omega}^{HB}_{bI} \times \mathbf{GH}^{HB} \tag{5}$$

Where $\times$ denotes the cross product between two vectors. Here the first term on the RHS of Eq (5) is zero since the hub center H is fixed in body frame F_b. We further can express the second term on the RHS of Eq (5) as

$$\mathbf{\Omega}^{HB}_{bI} \times \mathbf{GH}^{HB} = \left(\mathbb{T}_{(HB)b}\mathbf{\Omega}^b_{bI}\right) \times \left(\mathbb{T}_{(HB)b}\mathbf{GH}^b\right) \tag{6}$$

Since the earth is fixed, we obtain

$$\left(\frac{d\mathbf{GH}^I}{dt}\right)^{HB} = \left(\mathbb{T}_{(HB)b}\begin{pmatrix} p \\ q \\ r \end{pmatrix}\right) \times \left(\mathbb{T}_{(HB)b}\begin{pmatrix} x_H \\ y_H \\ z_H \end{pmatrix}^b\right) \tag{7}$$

For the third term on the RHS of Eq (3) we have

$$\begin{aligned} \left(\frac{d\mathbf{HP_{dm}}^I}{dt}\right)^{HB} &= \left(\frac{d\mathbf{HP_{dm}}^{HB}}{dt}\right)^{HB} + \mathbf{\Omega}^{HB}_{(HB)I} \times \mathbf{HP_{dm}}^{HB} \\ &= \frac{d}{dt}\begin{pmatrix} x_{dm} \\ y_{dm} \\ z_{dm} \end{pmatrix}^{HB} + \mathbf{\Omega}^{HB}_{(HB)I} \times \begin{pmatrix} x_{dm} \\ y_{dm} \\ z_{dm} \end{pmatrix}^{HB} \end{aligned} \tag{8}$$

With

$$\mathbf{\Omega}^{HB}_{(HB)I} = \mathbf{\Omega}^{HB}_{(HB)b} + \mathbf{\Omega}^{HB}_{bI} \tag{9}$$

And the first term on the RHS of Eq (9) is zero since frame F_{HB} is fixed wrt frame F_b. Additionally we have $\mathbf{\Omega}^{HB}_{bI} = \mathbb{T}_{(HB)b}\mathbf{\Omega}^{b}_{bI}$

Regrouping terms from Eq (4), Eq (7), Eq (8), and Eq (9), we can express the inertial velocity of a blade element dm in the Hub-Body frame F_{HB} as

$$\begin{aligned}\mathbf{V}^{HB}_{I,P_{dm}} &= \mathbb{T}_{(HB)b}.\mathbb{T}_{bo}\begin{pmatrix} V_N \\ V_E \\ V_Z \end{pmatrix}^{o} + \tfrac{d}{dt}\begin{pmatrix} x_{dm} \\ y_{dm} \\ z_{dm} \end{pmatrix}^{HB} \\ &+ \left(\mathbb{T}_{(HB)b}\begin{pmatrix} p \\ q \\ r \end{pmatrix}\right) \times \left(\mathbb{T}_{(HB)b}\begin{pmatrix} x_H \\ y_H \\ z_H \end{pmatrix}^{b} + \begin{pmatrix} x_{dm} \\ y_{dm} \\ z_{dm} \end{pmatrix}^{HB}\right)\end{aligned} \tag{10}$$

Since rotor shaft tilt-angles are zero, we get $\mathbb{T}_{(HB)b} = \mathbb{I}$. The expanded velocity expressions are further given in Appendix A.

IV. Flap-Lag Equations of Motion

The equations are obtained by the Lagrangian method,[19] which requires only velocity and position terms, and is much more convenient for overall system modeling. For an in-depth review of the flap-lag equations of motion, through the Lagrangian method, see Ref. 18, 27, 28. We have

$$\frac{d}{dt}\left(\frac{\partial K_E}{\partial \dot{\zeta_{bl}}}\right) - \frac{\partial K_E}{\partial \zeta_{bl}} = Q_{\zeta_{bl}} \tag{11a}$$

$$\frac{d}{dt}\left(\frac{\partial K_E}{\partial \dot{\beta_{bl}}}\right) - \frac{\partial K_E}{\partial \beta_{bl}} = Q_{\beta_{bl}} \tag{11b}$$

With K_E the kinetic energy of a rotor blade, ζ_{bl}, β_{bl} blade lag and flap angles, and $Q_{\zeta_{bl}}$, $Q_{\beta_{bl}}$ the generalized forces. These latter include the effect of gravity, aerodynamics, and spring damping and stiffness.

$$Q_{\zeta_{bl}} = Q_{\zeta_{bl},G} + Q_{\zeta_{bl},A} + Q_{\zeta_{bl},D} + Q_{\zeta_{bl},S} \tag{12a}$$

$$Q_{\beta_{bl}} = Q_{\beta_{bl},G} + Q_{\beta_{bl},A} + Q_{\beta_{bl},D} + Q_{\beta_{bl},S} \tag{12b}$$

The kinetic energy of a single rotor blade is given by

$$K_E = \frac{1}{2}\int_0^{R_{bl}} {\mathbf{V}^{HB}_{I,P_{dm}}}^{T}.\mathbf{V}^{HB}_{I,P_{dm}} dm \tag{13}$$

Where the limits of integration are from the flap hinge, i.e. *0*, to the blade tip, i.e. R_{bl}. The kinetic energy inboard of the flap hinge is neglected.

IV.A. Inertia Dynamics

We can rewrite the first term on the Left-Hand-Side (LHS) of Eq (11a) as

$$\frac{d}{dt}\left(\frac{\partial K_E}{\partial \dot{\zeta_{bl}}}\right) = \frac{d}{dt}\left(\frac{\partial}{\partial \dot{\zeta_{bl}}}\frac{1}{2}\int_0^{R_{bl}} {\mathbf{V}^{HB}_{I,P_{dm}}}^{T}.\mathbf{V}^{HB}_{I,P_{dm}} dm\right) \tag{14}$$

And since the limits of integration are constant, with Leibniz integral rule, the former expression is equal to

$$\frac{1}{2}\int_0^{R_{bl}} \frac{d}{dt}\frac{\partial}{\partial\dot{\zeta}_{bl}}\left(\mathbf{V}_{I,P_{dm}}^{HB\ T}.\mathbf{V}_{I,P_{dm}}^{HB}\right)dm \tag{15}$$

And Eq (15) is now equivalent to

$$\int_0^{R_{bl}} \frac{d}{dt}\left(\mathbf{V}_{I,P_{dm}}^{HB\ T}.\frac{\partial}{\partial\dot{\zeta}_{bl}}\mathbf{V}_{I,P_{dm}}^{HB}\right)dm = \int_0^{R_{bl}}\left[\mathbf{V}_{I,P_{dm}}^{HB\ T}.\frac{d}{dt}\frac{\partial}{\partial\dot{\zeta}_{bl}}\mathbf{V}_{I,P_{dm}}^{HB} + \frac{d}{dt}\left(\mathbf{V}_{I,P_{dm}}{}^{T}\right).\frac{\partial}{\partial\dot{\zeta}_{bl}}\mathbf{V}_{I,P_{dm}}^{HB}\right]dm \tag{16}$$

With

$$\frac{d}{dt}\frac{\partial}{\partial\dot{\zeta}_{bl}}\mathbf{V}_{I,P_{dm}}^{F_I} = \frac{d}{dt}\frac{\partial}{\partial\dot{\zeta}_{bl}}\mathbf{V}_{I,P_{dm}}^{HB} + \mathbf{\Omega}_{(HB)I}\times\frac{\partial}{\partial\dot{\zeta}_{bl}}\mathbf{V}_{I,P_{dm}} \tag{17}$$

We can rewrite the second term on the LHS of Eq (11a) as

$$-\frac{\partial K_E}{\partial\zeta_{bl}} = -\frac{\partial}{\partial\zeta_{bl}}\frac{1}{2}\int_0^{R_{bl}}\mathbf{V}_{I,P_{dm}}^{HB\ T}.\mathbf{V}_{I,P_{dm}}^{HB}dm \tag{18}$$

Again since the limits of integration are constant, we have

$$-\frac{1}{2}\int_0^{R_{bl}}\frac{\partial}{\partial\zeta_{bl}}\left(\mathbf{V}_{I,P_{dm}}^{HB\ T}.\mathbf{V}_{I,P_{dm}}^{HB}\right)dm = -\int_0^{R_{bl}}\mathbf{V}_{I,P_{dm}}^{HB\ T}.\frac{\partial}{\partial\zeta_{bl}}\mathbf{V}_{I,P_{dm}}^{HB}dm \tag{19}$$

Now summing the previous results we can provide an expression for the LHS of Eq (11a), i.e. the blade lead-lag equations of motion, as

$$\begin{aligned}\tfrac{d}{dt}\left(\tfrac{\partial K_E}{\partial\dot{\zeta}_{bl}}\right) - \tfrac{\partial K_E}{\partial\zeta_{bl}} &= \textstyle\int_0^{R_{bl}}\mathbf{V}_{I,P_{dm}}^{HB\ T}.\tfrac{d}{dt}\tfrac{\partial}{\partial\dot{\zeta}_{bl}}\mathbf{V}_{I,P_{dm}}^{HB}dm \\ &+ \textstyle\int_0^{R_{bl}}\tfrac{d}{dt}\left(\mathbf{V}_{I,P_{dm}}{}^{T}\right).\tfrac{\partial}{\partial\zeta_{bl}}\mathbf{V}_{I,P_{dm}}^{HB}dm - \int_0^{R_{bl}}\mathbf{V}_{I,P_{dm}}^{HB\ T}.\tfrac{\partial}{\partial\zeta_{bl}}\mathbf{V}_{I,P_{dm}}^{HB}dm\end{aligned} \tag{20}$$

Similarly for the flap equations of motion, the LHS of Eq (11b), we get

$$\begin{aligned}\tfrac{d}{dt}\left(\tfrac{\partial K_E}{\partial\dot{\beta}_{bl}}\right) - \tfrac{\partial K_E}{\partial\beta_{bl}} &= \textstyle\int_0^{R_{bl}}\mathbf{V}_{I,P_{dm}}^{HB\ T}.\tfrac{d}{dt}\tfrac{\partial}{\partial\dot{\beta}_{bl}}\mathbf{V}_{I,P_{dm}}^{HB}dm \\ &+ \textstyle\int_0^{R_{bl}}\tfrac{d}{dt}\left(\mathbf{V}_{I,P_{dm}}{}^{T}\right).\tfrac{\partial}{\partial\beta_{bl}}\mathbf{V}_{I,P_{dm}}^{HB}dm - \int_0^{R_{bl}}\mathbf{V}_{I,P_{dm}}^{HB\ T}.\tfrac{\partial}{\partial\beta_{bl}}\mathbf{V}_{I,P_{dm}}^{HB}dm\end{aligned} \tag{21}$$

Where the components of $\mathbf{V}_{I,P_{dm}}^{HB}$ are given in Appendix A. We can now reformulate Eq (11), using Eq (20) and Eq (21), to give the four-state nonlinear flap-lag equations of motion as follows

$$\frac{d}{dt}\begin{pmatrix}\dot{\beta}_{bl}\\ \dot{\zeta}_{bl}\\ \beta_{bl}\\ \zeta_{bl}\end{pmatrix} = \mathbb{A}^{-1}.\left(-\mathbb{B}.\begin{pmatrix}\dot{\beta}_{bl}\\ \dot{\zeta}_{bl}\\ \beta_{bl}\\ \zeta_{bl}\end{pmatrix} - \begin{pmatrix}F_1\\ F_2\\ 0\\ 0\end{pmatrix} + \begin{pmatrix}Q_{\beta_{bl}}\\ Q_{\zeta_{bl}}\\ 0\\ 0\end{pmatrix}\right) \tag{22}$$

With the following matrices

$$\mathbb{A} = \begin{bmatrix} I_\beta & 0 & 0 & 0 \\ 0 & (e_F^2.M_{bl} + 2e_F.C_0 + I_\beta) & 0 & 0 \\ 0 & 0 & 1 & 0 \\ 0 & 0 & 0 & 1 \end{bmatrix} \tag{23}$$

$$\mathbb{B} = \begin{bmatrix} 0 & B_{12} & 0 & 0 \\ B_{21} & 0 & 0 & 0 \\ -1 & 0 & 0 & 0 \\ 0 & -1 & 0 & 0 \end{bmatrix} \tag{24}$$

With M_{bl}, C_0, and I_β defined in Appendix A. Expressions B_{12}, B_{21}, F_1, and F_2 are lengthy expressions of $(\dot{\zeta_{bl}}\ \beta_{bl}\ \zeta_{bl})$. These B_i, and F_i expressions are further only valid for small flap, lag, and pitch angles and can be found in Ref. 29.

IV.B. Virtual Work and Virtual Displacements

The determination of the generalized forces requires the calculation of the virtual work of an individual external force, associated with its respective virtual flapping and lead-lag displacements.[18] Let $F_{X_i}, F_{Y_i}, F_{Z_i}$ be the components of the *ith* external force $\mathbf{F}_i$, acting on blade element dm in frame F_{HB}, then the resulting elemental virtual work done by this force, and due to the virtual flapping and lag displacements $\partial\beta_{bl}$ and $\partial\zeta_{bl}$, is given by

$$dW_i = F_{X_i} dx_{dm} + F_{Y_i} dy_{dm} + F_{Z_i} dz_{dm} \tag{25}$$

$$dx_{dm} = \frac{\partial x_{dm}}{\partial \beta_{bl}} \partial\beta_{bl} + \frac{\partial x_{dm}}{\partial \zeta_{bl}} \partial\zeta_{bl} \tag{26a}$$

$$dy_{dm} = \frac{\partial y_{dm}}{\partial \beta_{bl}} \partial\beta_{bl} + \frac{\partial y_{dm}}{\partial \zeta_{bl}} \partial\zeta_{bl} \tag{26b}$$

$$dz_{dm} = \frac{\partial z_{dm}}{\partial \beta_{bl}} \partial\beta_{bl} + \frac{\partial z_{dm}}{\partial \zeta_{bl}} \partial\zeta_{bl} \tag{26c}$$

Now summing up the elemental virtual work, over the appropriate blade span, results in the total virtual work W_i due to external force $\mathbf{F}_i$

$$\begin{aligned} W_i \quad &= \int_0^{R_{bl}} \left(F_{X_i} \tfrac{\partial x_{dm}}{\partial \beta_{bl}} + F_{Y_i} \tfrac{\partial y_{dm}}{\partial \beta_{bl}} + F_{Z_i} \tfrac{\partial z_{dm}}{\partial \beta_{bl}} \right) \partial\beta_{bl} \\ &+ \int_0^{R_{bl}} \left(F_{X_i} \tfrac{\partial x_{dm}}{\partial \zeta_{bl}} + F_{Y_i} \tfrac{\partial y_{dm}}{\partial \zeta_{bl}} + F_{Z_i} \tfrac{\partial z_{dm}}{\partial \zeta_{bl}} \right) \partial\zeta_{bl} \end{aligned} \tag{27}$$

Which is equivalent to

$$W_i = Q_{\beta_{bl},i}.\partial\beta_{bl} + Q_{\zeta_{bl},i}.\partial\zeta_{bl} \tag{28}$$

The virtual displacement, in the Hub-Body frame, of a blade element outboard of the flap hinge is obtained, using Eq (26) and Eq (1) as follows

$$\begin{pmatrix} dx_{dm} \\ dy_{dm} \\ dz_{dm} \end{pmatrix}^{HB} = r_{dm}.\mathbf{dP}^{HB}_{\beta,r}.\partial\beta_{bl} + r_{dm}.\mathbf{dP}^{HB}_{\zeta,r}.\partial\zeta_{bl} + \mathbf{dP}^{HB}_{\zeta,\bar{r}}.\partial\zeta_{bl} \tag{29}$$

With

$$\mathbf{dP}^{HB}_{\beta,r} = \begin{pmatrix} \cos\psi_{bl}\cos\zeta_{bl}\sin\beta_{bl} + \sin\psi_{bl}\Big(\cos\theta_{bl}\sin\zeta_{bl}\sin\beta_{bl} - \cos\beta_{bl}\sin\theta_{bl}\Big) \\ \Gamma\Big(\cos\psi_{bl}\Big(\cos\theta_{bl}\sin\zeta_{bl}\sin\beta_{bl} - \cos\beta_{bl}\sin\theta_{bl}\Big) - \sin\psi_{bl}\cos\zeta_{bl}\sin\beta_{bl}\Big) \\ -\cos\theta_{bl}\cos\beta_{bl} - \sin\zeta_{bl}\sin\theta_{bl}\sin\beta_{bl} \end{pmatrix} \tag{30}$$

$$\mathbf{dP}^{HB}_{\zeta,r} = \cos\beta_{bl}\begin{pmatrix} \Big(\cos\psi_{bl}\sin\zeta_{bl} - \sin\psi_{bl}\cos\theta_{bl}\cos\zeta_{bl}\Big) \\ -\Gamma\Big(\cos\psi_{bl}\cos\theta_{bl}\cos\zeta_{bl} + \sin\psi_{bl}\sin\zeta_{bl}\Big) \\ \cos\zeta_{bl}\sin\theta_{bl} \end{pmatrix} \tag{31}$$

$$\mathbf{dP}^{HB}_{\zeta,\bar{r}} = e_F\begin{pmatrix} \Big(\cos\psi_{bl}\sin\zeta_{bl} - \sin\psi_{bl}\cos\theta_{bl}\cos\zeta_{bl}\Big) \\ -\Gamma\Big(\cos\psi_{bl}\cos\theta_{bl}\cos\zeta_{bl} + \sin\psi_{bl}\sin\zeta_{bl}\Big) \\ \cos\zeta_{bl}\sin\theta_{bl} \end{pmatrix} \tag{32}$$

IV.C. Generalized Forces: Gravity

The gravity force acting on a blade element with mass dm can be expressed in the Hub-Body frame F_{HB} as

$$\mathbf{F}^{HB}_{G_{bl}} = \mathbb{T}_{(HB)o}\begin{pmatrix} 0 \\ 0 \\ g.dm \end{pmatrix}^{o} \tag{33}$$

Substituting Eq (33) and Eq (29) into Eq (27), the desired generalized forces due to gravity, outboard of the flap hinge, are obtained as follows

$$\begin{aligned} Q_{\beta_{bl},G} \quad &= g.C_0.\Big(A_1\cos\psi_{bl}\cos\zeta_{bl}\sin\beta_{bl} + A_1\sin\psi_{bl}\cos\theta_{bl}\sin\zeta_{bl}\sin\beta_{bl} \\ &\quad -A_1\sin\psi_{bl}\cos\beta_{bl}\sin\theta_{bl} + A_2\Gamma\cos\psi_{bl}\cos\theta_{bl}\sin\zeta_{bl}\sin\beta_{bl} \\ &\quad -A_2\Gamma\cos\psi_{bl}\cos\beta_{bl}\sin\theta_{bl} - A_2\Gamma\sin\psi_{bl}\cos\zeta_{bl}\sin\beta_{bl} \\ &\quad -A_3\cos\theta_{bl}\cos\beta_{bl} - A_3\sin\zeta_{bl}\sin\theta_{bl}\sin\beta_{bl}\Big) \end{aligned} \tag{34}$$

$$\begin{aligned} Q_{\zeta_{bl},G} \quad &= g.\Big(e_F.M_{bl} + C_0\cos\beta_{bl}\Big).\Big(A_1\cos\psi_{bl}\sin\zeta_{bl} - A_1\sin\psi_{bl}\cos\theta_{bl}\cos\zeta_{bl} \\ &\quad -A_2\Gamma\cos\psi_{bl}\cos\theta_{bl}\cos\zeta_{bl} - A_2\Gamma\sin\psi_{bl}\sin\zeta_{bl} + A_3\cos\zeta_{bl}\sin\theta_{bl}\Big) \end{aligned} \tag{35}$$

And

$$\begin{aligned} A_1 &= -\sin\theta \\ A_2 &= \cos\theta\sin\phi \\ A_3 &= \cos\theta\cos\phi \end{aligned} \tag{36}$$

With M_{bl} and C_0 defined in Appendix A.

IV.D. Generalized Forces: Hub Damping and Hub Spring Restraints

We consider hinge springs with viscous dampers. The generalized forces corresponding to the spring dampers can be obtained directly from the potential energy of the hub dampers dissipation functions.[18,19]

$$Q_{\zeta_{bl},D} = -K_{D_\zeta}.\dot{\zeta_{bl}} \tag{37}$$

$$Q_{\beta_{bl},D} = -K_{D_\beta}.\dot{\beta_{bl}} \tag{38}$$

Similarly the generalized forces corresponding to the spring restraints can be obtained directly from the potential energy of the hub springs.[18,19]

$$Q_{\zeta_{bl},S} = -K_{S_\zeta}.\zeta_{bl} \tag{39}$$

$$Q_{\beta_{bl},S} = -K_{S_\beta}.(\beta_{bl} - \beta_P) \tag{40}$$

Where we have subtracted the precone angle β_P, see Ref. 3. Here an approximation is made since we have neglected the effect of the precone angle in the LHS of the flap-lag equations of motion.

IV.E. Generalized Forces: Aerodynamic

IV.E.1. Blade element velocities

The flow velocities perpendicular and tangential to the reference frame F_{ref} are named U_P and U_T, see figure 3. They represent the velocities of a blade element dm as if it were fixed in space, while the air flows around it.

$$U_P = \begin{pmatrix} 0 \\ 0 \\ 1 \end{pmatrix}^T .\mathbb{T}_{(ref)(HB)}.\left(-\mathbf{V}_{a,G}^{HB} + \mathbb{T}_{(HB)(TPP)} \begin{pmatrix} 0 \\ 0 \\ v_i \end{pmatrix}^{TPP} \right) \tag{41}$$

$$U_T = -\begin{pmatrix} 1 \\ 0 \\ 0 \end{pmatrix}^T .\mathbb{T}_{(ref)(HB)}.\mathbf{V}_{a,G}^{HB} \tag{42}$$

$$\mathbf{V}_{a,G}^{HB} = \begin{pmatrix} u_{I,P_{dm}} \\ v_{I,P_{dm}} \\ w_{I,P_{dm}} \end{pmatrix}^{HB} - \mathbb{T}_{(HB)o} \begin{pmatrix} u_w \\ v_w \\ w_w \end{pmatrix}^o \tag{43}$$

With v_i the rotor induced velocity. Further $u_{I,P_{dm}}^{HB}$, $v_{I,P_{dm}}^{HB}$, and $w_{I,P_{dm}}^{HB}$ are given in Appendix A, and u_w^o, v_w^o, and w_w^o are the components of the wind velocity vector in frame F_o.

IV.E.2. Elementary Forces

Here we consider the flow over a blade element, this is why the accompanying theory is named blade element method/theory. The magnitude of the elementary lift and drag forces can be written as

$$dL_{bl} = K_{defic}.\frac{1}{2}\rho.U^2.c_{l_{bl}}.c_{bl}.dr_{dm} \tag{44}$$

$$dD_{bl} = \frac{1}{2}\rho.U^2.c_{d_{bl}}.c_{bl}.dr_{dm} \tag{45}$$

With the flow velocity $U = \sqrt{U_T^2 + U_P^2}$, and the blade section lift and drag coefficients $c_{l_{bl}}$ and $c_{d_{bl}}$ given as tabulated functions[g] of blade section angle of attack $\alpha_{bl} = \theta_{bl} - \phi_{bl}$ and Mach number $M = \frac{U}{a}$. We can express now the elementary lift and drag forces in frame F_{ref} as

$$\mathbf{dL}_{bl}^{ref} = sign(U_T).dL_{bl}.\begin{pmatrix} \sin\phi_{bl} \\ 0 \\ \Gamma\cos\phi_{bl} \end{pmatrix} \tag{46}$$

$$\mathbf{dD}_{bl}^{ref} = dD_{bl}.\begin{pmatrix} -\Gamma\cos\phi_{bl} \\ 0 \\ \sin\phi_{bl} \end{pmatrix} \tag{47}$$

Finally blade pitch θ_{bl}, see Ref. 18, and inflow angle ϕ_{bl} are given next as

$$\theta_{bl} = \theta_{0_{bl}} + \theta_{1c_{bl}}\cos(\psi_{bl} + \psi_{PA}) + \theta_{1s_{bl}}\sin(\psi_{bl} + \psi_{PA}) + \theta_{t,r_{dm}} - K_{(\theta\beta)}.\beta_{bl} - K_{(\theta\zeta)}.\zeta_{bl} \tag{48}$$

$$\begin{aligned} &CCW \Rightarrow \Gamma = 1 \\ &\phi_{bl} = -\arctan\tfrac{U_P}{U_T} \quad \text{if} \quad U_T < 0 \\ &\phi_{bl} = sign(U_P).\tfrac{\pi}{2} + \arctan\tfrac{U_T}{U_P} \quad \text{if} \quad 0 \leq U_T \end{aligned} \tag{49}$$

$$\begin{aligned} &CW \Rightarrow \Gamma = -1 \\ &\phi_{bl} = \arctan\tfrac{U_P}{U_T} \quad \text{if} \quad 0 < U_T \\ &\phi_{bl} = sign(U_P).\tfrac{\pi}{2} - \arctan\tfrac{U_T}{U_P} \quad \text{if} \quad U_T \leq 0 \end{aligned} \tag{50}$$

IV.E.3. Generalized Forces

The generalized aerodynamic force due to blade lead-lag was given in Eq (12). We express this latter as the sum of two contributions, one due to lift Q_{ζ_{bl},A_L}, and one due to drag Q_{ζ_{bl},A_D}, hence $Q_{\zeta_{bl},A} = Q_{\zeta_{bl},A_L} + Q_{\zeta_{bl},A_D}$. Now keeping in mind Eq (27), and using Eq (31), and Eq (32) we obtain

$$Q_{\zeta_{bl},A_L} = \int_{r_c}^{B.R_{bl}} \left(\mathbb{T}_{(HB)(ref)}\mathbf{dL}_{bl}^{ref}\right)^T.\left(r_{dm}.\mathbf{dP}_{\zeta,r}^{HB} + \mathbf{dP}_{\zeta,\bar{r}}^{HB}\right).dr_{dm} \tag{51}$$

[g]Where we neglect sideslip influence.

$$Q_{\zeta_{bl},A_D} = \int_{r_c}^{R_{bl}} \left(\mathbb{T}_{(HB)(ref)} \mathbf{dD}_{bl}^{ref} \right)^T . \left(r_{dm} . \mathbf{dP}_{\zeta,r}^{HB} + \mathbf{dP}_{\zeta,\bar{r}}^{HB} \right) . dr_{dm} \tag{52}$$

For the lift contribution, the integration is performed from the blade root cutout r_c to a value denoted as $B.R_{bl}$, this latter accounts for blade tip loss.[30]

Similarly for the generalized forces due to the blade flap contribution $Q_{\beta_{bl},A} = Q_{\beta_{bl},A_L} + Q_{\beta_{bl},A_D}$, we get

$$Q_{\beta_{bl},A_L} = \int_{r_c}^{B.R_{bl}} \left(\mathbb{T}_{(HB)(ref)} \mathbf{dL}_{bl}^{ref} \right)^T . \mathbf{dP}_{\beta,r}^{HB} . r_{dm} . dr_{dm} \tag{53}$$

$$Q_{\beta_{bl},A_D} = \int_{r_c}^{R_{bl}} \left(\mathbb{T}_{(HB)(ref)} \mathbf{dD}_{bl}^{ref} \right)^T . \mathbf{dP}_{\beta,r}^{HB} . r_{dm} . dr_{dm} \tag{54}$$

Now providing analytical expressions for the previous four integrals represents a rather tedious task, even more so for twisted blades[h] for which the blade pitch will also be function of the distance r_{dm}. Therefore we have opted for a numerical evaluation of these expressions, as is often done in flight dynamics codes.[31] Here Gaussian quadrature integration was implemented, using a low order (fifth order) Legendre polynomial scheme.[20,21]

IV.F. Flap Angle as a Fourier Series

Blade motion is 2π periodic around the azimuth and may hence be expanded as an infinite Fourier series.[3,24] Now for full-scale helicopters, it is well known that the magnitude of the flap second harmonic are less than 10% the magnitude of the flap first harmonic.[24,32] We assume that this is also the case for small-scale helicopters. Therefore we neglect second and higher harmonics in the Fourier series

$$\beta_{bl}(\psi_{bl}) \simeq \beta_0 + \beta_{1c} \cos\psi_{bl} + \beta_{1s} \sin\psi_{bl} \tag{55}$$

The first harmonic representation of the blade motion defines the rotor Tip-Path-Plane (TPP). This type of motion results in a cone-shaped rotor. The non-periodic term β_0 describes the so-called coning angle, and the coefficients of the first harmonic β_{1c} and β_{1s} describe the tilting of the rotor TPP, in the longitudinal and lateral directions respectively. Now in steady-state rotor operation, the flap coefficients β_0, β_{1c}, β_{1s} may be considered constant over a 2π blade revolution. Hence a steady-state periodic solution in the form of a Fourier series as given in Eq (55) may be found through least-squares.[33] Obviously this solution would not be adequate for transient situations such as maneuvering,[30] hence in our model we compute for each new blade azimuth the instantaneous TPP angles.

V. Simulation Results

We compare time-response outputs from our model, implemented in a MATLAB® environment,[34] and those from an equivalent FLIGHTLAB[35] rotor model, for the case of a R/C helicopter flybarless hub, for which the main physical dimensions have been given in Appendix C. In this paper we only provide visual comparisons of data for blade flap/lag angles β_{bl}, ζ_{bl}, flap/lag rotational velocities $\dot{\beta}_{bl}, \dot{\zeta}_{bl}$, and the three TPP angles $\beta_0, \beta_{1c}, \beta_{1s}$. The test is organized as follows. First, the rotor is allowed to reach a steady-state condition during a time period of 0.5s. Then, for the following 3s, we simultaneously apply a sinusoid of 1° in amplitude at a frequency of 2Hz[i] on collective, lateral and longitudinal cyclics. The first test is run from a hover trim condition, see figure 4 and figure 5, while the second test is run to check the high speed flight

[h] Although in our case we have assumed zero twist.

[i] Corresponding to the maximum anticipated closed-loop system bandwidth for autonomous flight.

characteristics, see figure 6 and figure 7. In table 1 we provide the maximum absolute amplitude deviations between our model and FLIGHTLAB.

We discuss first the amplitude match. For the flap angle the match with FLIGHTLAB is very good in hover as $|\Delta_{max}| = 0.4°$ and good at $u = 10$ m/s with $|\Delta_{max}| = 0.7°$, while the lag angle match is very good for both test cases. Furthermore, although the lag velocity match is rather good for both test cases, we see that the flap velocity match deteriorates from hover to $u = 10$ m/s. Finally for the longitudinal/lateral TPP angles the match with FLIGHTLAB is again very good in hover as $|\Delta_{max}| = 0.2 - 0.35°$ and good at $u = 10$ m/s with $|\Delta_{max}| = 0.7°$, while the coning angle match is good for both test cases.

Now concerning the frequency content of these seven variables, and based on visual comparisons, we see that for both test conditions the fit is very good for flap, lag and TPP angles, and good for the lag velocity, while the fit for the flap velocity deteriorates as the body longitudinal velocity u increases. These observed differences, between our model and FLIGHTLAB at high speed, are a subject of ongoing research.

Name	Unit	Hover $\lvert\Delta_{max}\rvert$	High Speed ($u = 10$ m/s) $\lvert\Delta_{max}\rvert$
Flap	°	0.4	0.7
Lag	°	0.18	0.18
Flap velocity	°/s	40	114
Lag velocity	°/s	3.5	6.4
Coning TPP	°	0.55	0.5
Longitudinal TPP	°	0.2	0.7
Lateral TPP	°	0.35	0.7

Table 1. Maximum absolute amplitude deviations between model and FLIGHTLAB

VI. Conclusion

We have presented the coupled flap-lag equations of motion, for a small-scale helicopter flybarless rotor, in the case of a rigid articulated Pitch-Lag-Flap (P-L-F) hinge arrangement. The (P-L-F) sequence is indeed much more useful for modeling the rotor dynamics of R/C helicopters. The model has been compared with an equivalent FLIGHTLAB rotor model, in hover and at high speed. The amplitude and frequency match for the flap, lag, and TPP angles is good to very good for both test conditions, while the amplitude and frequency match of flap and lag velocities is good in hover and fair at high speed. While keeping in mind the model's accuracy reduction at high speed, the present blade flap-lag model could potentially be integrated into a small-scale helicopter flight dynamics simulation environment, for the purpose of research and development of high bandwidth control systems.

Appendix A: Additional Expressions

The inertial velocity x-y-z-components, in F_{HB}, of an element dm are given next, and are valid for both CW and CCW rotors through the switch Γ.

$$
\begin{aligned}
u^{HB}_{I,P_{dm}} = u + \Omega_{MR}\Big(& \sin\psi_{bl}[e_L + e_P + \cos\zeta_{bl}(e_F + r_{dm}\cos\beta_{bl})] \\
& - \cos\psi_{bl}[\cos\theta_{bl}\sin\zeta_{bl}(e_F + r_{dm}\cos\beta_{bl}) + r_{dm}\sin\beta_{bl}\sin\theta_{bl}]\Big) \\
& + \dot{\zeta_{bl}}(e_F + r_{dm}\cos\beta_{bl})[\cos\psi_{bl}\sin\zeta_{bl} - \sin\psi_{bl}\cos\theta_{bl}\cos\zeta_{bl}] \\
& + \dot{\beta_{bl}} r_{dm}[\cos\psi_{bl}\cos\zeta_{bl}\sin\beta_{bl} + \sin\psi_{bl}(\cos\theta_{bl}\sin\zeta_{bl}\sin\beta_{bl} - \cos\beta_{bl}\sin\theta_{bl})] \\
& + \dot{\theta_{bl}}\sin\psi_{bl}[\sin\theta_{bl}\sin\zeta_{bl}(e_F + r_{dm}\cos\beta_{bl}) - r_{dm}\sin\beta_{bl}\cos\theta_{bl}] \\
& + q\Big(z_H - r_{dm}\cos\theta_{bl}\sin\beta_{bl} + (e_F + r_{dm}\cos\beta_{bl})\sin\zeta_{bl}\sin\theta_{bl}\Big) \\
& - r\Big(y_H - \Gamma\cos\psi_{bl}(\cos\theta_{bl}\sin\zeta_{bl}(e_F + r_{dm}\cos\beta_{bl}) \\
& + r_{dm}\sin\beta_{bl}\sin\theta_{bl}) + \Gamma\sin\psi_{bl}(e_L + e_P + \cos\zeta_{bl}(e_F + r_{dm}\cos\beta_{bl}))\Big)
\end{aligned}
$$

$$
\begin{aligned}
v^{HB}_{I,P_{dm}} = v + \Omega_{MR}\Gamma\Big(& (e_L + e_P)\cos\psi_{bl} + r_{dm}\sin\psi_{bl}\sin\beta_{bl}\sin\theta_{bl} \\
& + (e_F + r_{dm}\cos\beta_{bl})(\cos\psi_{bl}\cos\zeta_{bl} + \sin\psi_{bl}\cos\theta_{bl}\sin\zeta_{bl})\Big) \\
& - \dot{\zeta_{bl}}\Gamma(e_F + r_{dm}\cos\beta_{bl})[\cos\psi_{bl}\cos\zeta_{bl}\cos\theta_{bl} + \sin\psi_{bl}\sin\zeta_{bl}] \\
& + \dot{\beta_{bl}} r_{dm}\Gamma(\cos\psi_{bl}\cos\theta_{bl}\sin\zeta_{bl}\sin\beta_{bl} - \cos\psi_{bl}\cos\beta_{bl}\sin\theta_{bl} - \sin\psi_{bl}\cos\zeta_{bl}\sin\beta_{bl}) \\
& + \dot{\theta_{bl}}\Gamma\cos\psi_{bl}[\sin\theta_{bl}\sin\zeta_{bl}(e_F + r_{dm}\cos\beta_{bl}) - r_{dm}\sin\beta_{bl}\cos\theta_{bl}] \\
& - p\Big(z_H - \Big(r_{dm}\cos\theta_{bl}\sin\beta_{bl} - (e_F + r_{dm}\cos\beta_{bl})\sin\zeta_{bl}\sin\theta_{bl}\Big)\Big) \\
& + r\Big(x_H - \Big(\cos\psi_{bl}(e_L + e_P + \cos\zeta_{bl}(e_F + r_{dm}\cos\beta_{bl})) \\
& + \sin\psi_{bl}(\cos\theta_{bl}\sin\zeta_{bl}(e_F + r_{dm}\cos\beta_{bl}) + r_{dm}\sin\beta_{bl}\sin\theta_{bl})\Big)\Big)
\end{aligned}
$$

$$
\begin{aligned}
w^{HB}_{I,P_{dm}} = w &+ \dot{\zeta_{bl}} \cos\zeta_{bl} \sin\theta_{bl}(e_F + r_{dm}\cos\beta_{bl}) \\
&- \dot{\beta_{bl}} r_{dm}(\cos\beta_{bl}\cos\theta_{bl} + \sin\beta_{bl}\sin\zeta_{bl}\sin\theta_{bl}) \\
&+ \dot{\theta_{bl}}[r_{dm}\sin\theta_{bl}\sin\beta_{bl} + (e_F + r_{dm}\cos\beta_{bl})\sin\zeta_{bl}\cos\theta_{bl}] \\
&+ p\Big(y_H - \Gamma\cos\psi_{bl}(\cos\theta_{bl}\sin\zeta_{bl}(e_F + r_{dm}\cos\beta_{bl}) + r_{dm}\sin\beta_{bl}\sin\theta_{bl}) \\
&\quad + \Gamma\sin\psi_{bl}(e_L + e_P + \cos\zeta_{bl}(e_F + r_{dm}\cos\beta_{bl}))\Big) \\
&- q\Big(x_H - \cos\psi_{bl}(e_L + e_P + \cos\zeta_{bl}(e_F + r_{dm}\cos\beta_{bl})) \\
&\quad - \sin\psi_{bl}(\cos\theta_{bl}\sin\zeta_{bl}(e_F + r_{dm}\cos\beta_{bl}) + r_{dm}\sin\beta_{bl}\sin\theta_{bl})\Big)
\end{aligned}
$$

Assuming a blade constant mass distribution per unit length we also have

$$
\begin{aligned}
&M_{bl} = \int_0^{R_{bl}} dm \qquad C_0 = \int_0^{R_{bl}} r_{dm}.dm = M_{bl}.y_{G_{bl}} \\
&I_\beta = \int_0^{R_{bl}} r^2_{dm}.dm = M_{bl}.\tfrac{R^2_{bl}}{3} \qquad C_1 = \int_0^{R_{bl}} r^3_{dm}.dm = M_{bl}.\tfrac{R^3_{bl}}{4}
\end{aligned}
$$

Appendix B: Frames

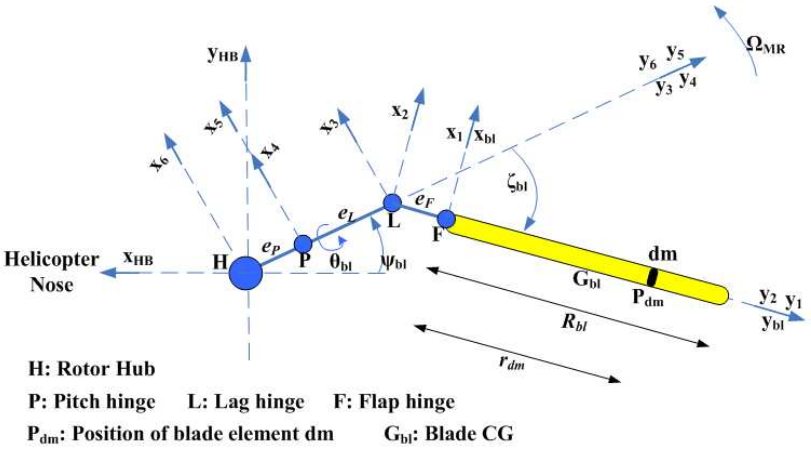

Figure 1. Main rotor frames (top-view)

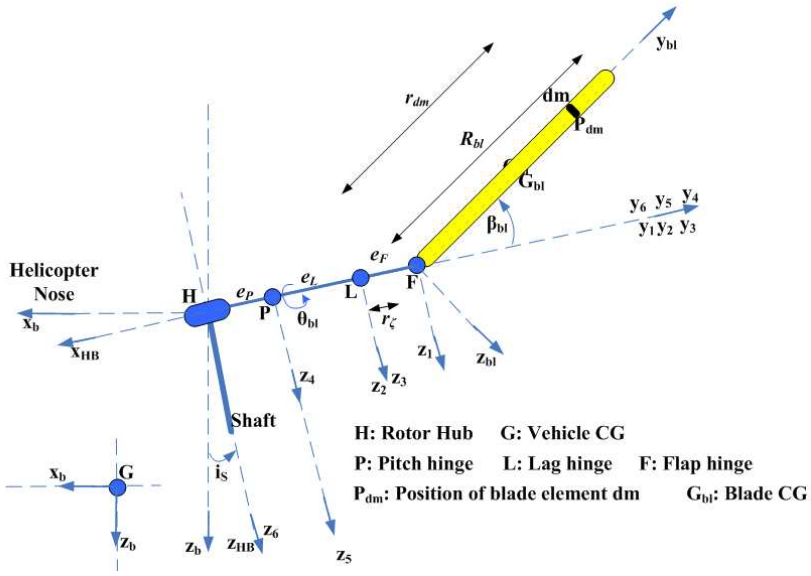

Figure 2. Main rotor frames (side-view)

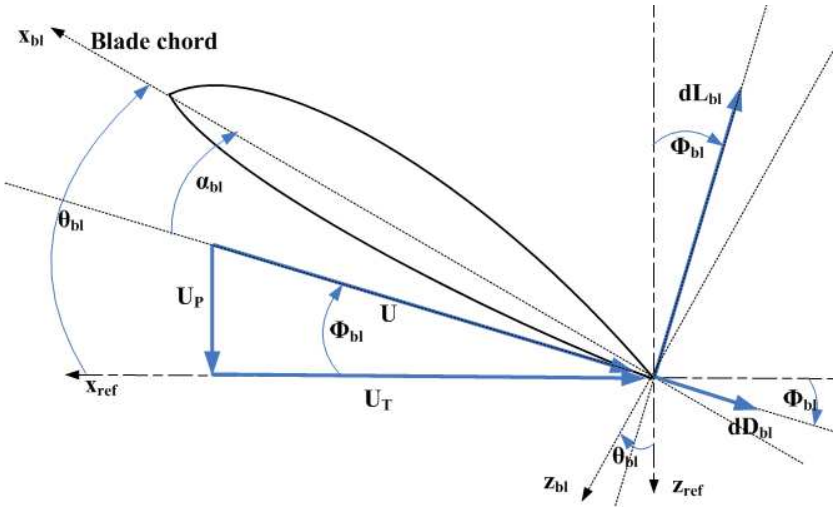

Figure 3. Elemental aerodynamic forces (CCW). View from an observer positioned on rotor shaft, and looking outboard at an advancing blade

Appendix C: Rotor Physical Parameters

Name	Parameter	Value	Unit
Airfoil lift/drag coef.	$c_{l_{bl}}$, $c_{d_{bl}}$	NACA0012	
Blade chord	c_{bl}	0.076	m
Blade mass	M_{bl}	0.277	kg
Hub arm chord	c_{hub}	0.015	m
Number of blades	N_b	2	
Nominal angular velocity	$\Omega_{MR_{100\%}}$	151.843	rad/s
Offset distance	e_P	0.035	m
Offset distance	e_L	0.049	m
Offset distance	e_F	0.010	m
Pitch-flap coupling ratio	$K_{(\theta\beta)}$	0	
Pitch-lag coupling ratio	$K_{(\theta\zeta)}$	0	
Precone angle	β_P	0	rad
Root cutout from flap hinge	r_c	0.006	m
Rotor radius from hub	R_{rot}	0.944	m
Spring restraint coef. due to flap	K_{S_β}	271.1635	$N.m/rad$
Spring damping coef. due to flap	K_{D_β}	0	$N.m.s/rad$
Spring restraint coef. due to lag	K_{S_ζ}	0	$N.m/rad$
Spring damping coef. due to lag	K_{D_ζ}	24.4047	$N.m.s/rad$
Swashplate phase angle	ψ_{PA}	0	rad
Tip loss factor	B	0.97	
Y-pos. blade CG wrt flap hinge	$y_{G_{bl}}$	0.8932	m

Appendix D: Comparisons with FLIGHTLAB

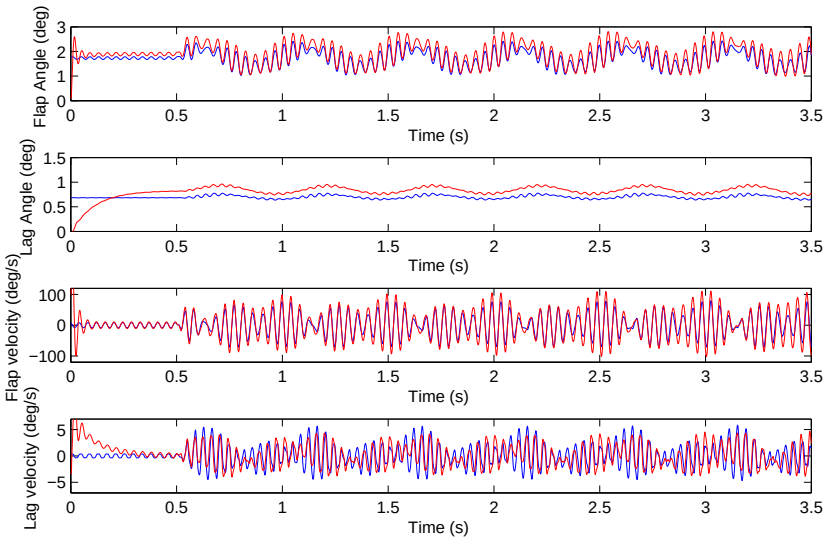

Figure 4. Flap/Lag angles & velocities, starting at hover (–FLIGHTLAB –Model)

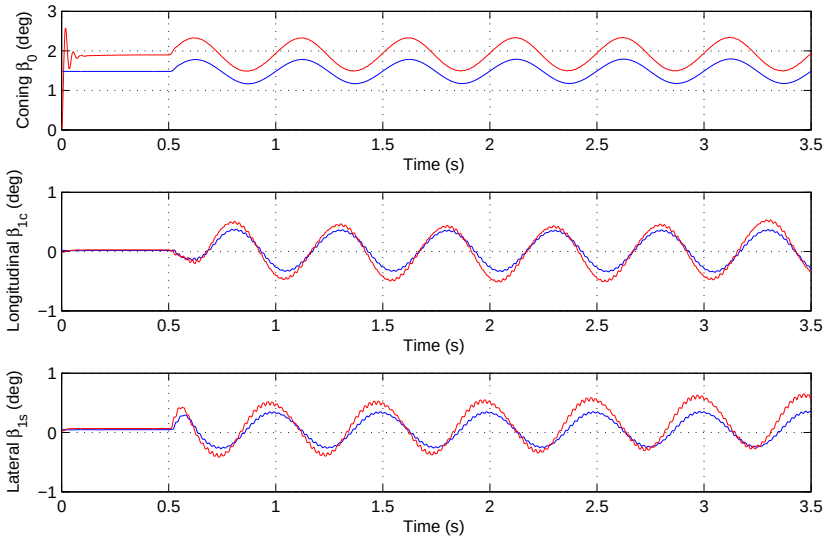

Figure 5. TPP angles, starting at hover (–FLIGHTLAB –Model)

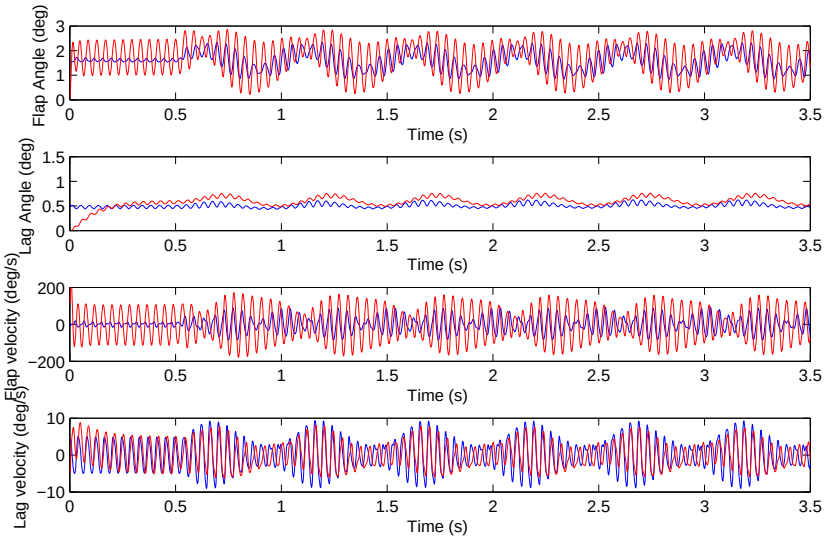

Figure 6. Flap/Lag angles & velocities, starting at $u = 10$ m/s (–FLIGHTLAB –Model)

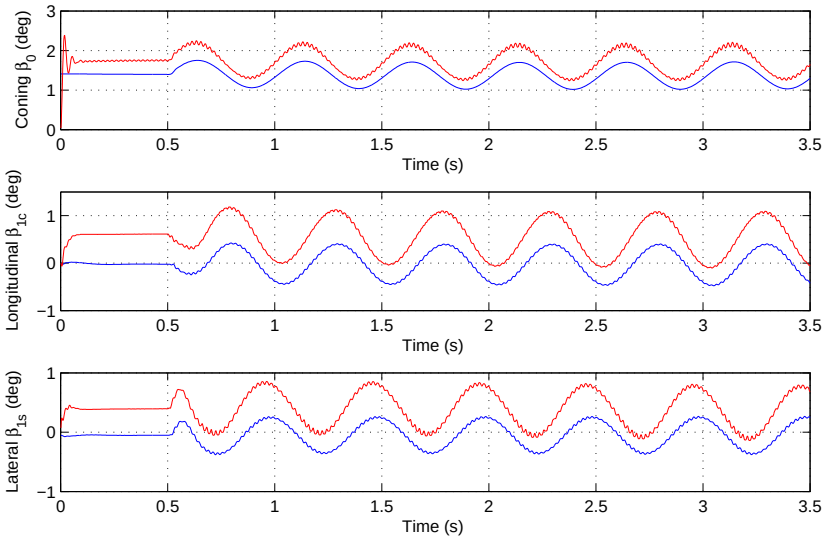

Figure 7. TPP angles, starting at $u = 10$ m/s (–FLIGHTLAB –Model)

References

[1]Boiffier, J. L., *The Dynamics of Flight The Equations*, John Wiley & Sons, Chichester, England, 1998.

[2]Mansur, M. H., Tischler, M. B., Chaimovich, M., Rosen, A., and Rand, O., "Modeling Methods for High-Fidelity Rotorcraft Flight Mechanics Simulation," Tech. Rep. TM 103842, NASA Ames Research Center, 1992.

[3]Johnson, W., *Helicopter Theory*, Dover Publications Inc., NY, USA, 1994.

[4]Blake, B. B. and Lunn, K., "Helicopter Stability and Control Test Methodology," *AIAA Atmospheric Flight Mechanics Conference*, 1980.

[5]Ellis, C. W., "Effects of Rotor Dynamics on Helicopter Automatic Control System Requirements," *Aeronautical Engineering Review*, 1953.

[6]Hall, W. E. and Bryson, A. E., "Inclusion of Rotor Dynamics in Controller Design for Helicopters," *AIAA Journal of Aircraft*, Vol. 10, No. 4, 1973, pp. 200–206.

[7]Miyajima, K., "Analytical Design of a High Performance Stability and Control Augmentation System for a Hingeless Rotor Helicopter," *Journal of the American Helicopter Society*, 1979.

[8]Chen, R. T. N., "Effects of Primary Rotor Parameters on Flapping Dynamics," Tech. Rep. NTP 1431, NASA Ames Research Center, 1980.

[9]Chen, R. T. N. and Hindson, W. S., "Influence of High-Order Dynamics on Helicopter Flight Control System Bandwidth," *AIAA Journal of Guidance, Control, and Dynamics*, Vol. 9, No. 2, 1986, pp. 190–197.

[10]Curtiss, H. C., "Stability and Control Modeling," *12th European Rotorcraft Forum*, 1986.

[11]Brinson, P. R., "Towards Higher Bandwidth in Helicopter Flight Control Systems," *Royal Aeronautical Society Conference on Helicopter Handling Qualities and Control*, 1988.

[12]Curtiss, H. C., "Physical Aspects of Rotor Body Coupling in Stability and Control," *46th Annual Forum of the American Helicopter Society*, 1990.

[13]Miller, D. G. and White, F., "A Treatment of the Impact of Rotor-Fuselage Coupling on Helicopter Handling Qualities," *43rd Annual Forum of the American Helicopter Society*, 1987.

[14]Tischler, M. B., "System Identification Requirements for High Bandwidth Rotorcraft Flight Control System Design," *AGARD LS-178 Rotorcraft System Identification*, 1991.

[15]Padfield, G. D., *Helicopter Flight Dynamics*, Blackwell Science Ltd, Oxford, UK, 1996.

[16]Brackbill, C. R., *Helicopter Rotor Aeroelastic Analysis Using a Refined Elastomeric Damper Model*, Ph.D. thesis, Pennsylvania State University, 2000.

[17]Manimala, B., Walker, D., and Padfield, G., "Rotorcraft Simulation modeling and Validation for Control Design and Load Prediction," *31st European Rotorcraft Forum*, 2005.

[18]Chen, R. T. N., "Flap-Lag Equations of Motion of Rigid, Articulated Rotor Blades with Three Hinge Sequences," Tech. Rep. NTM 100023, NASA Ames Research Center, 1987.

[19]Wells, D. A., *Lagrangian Dynamics*, McCraw-Hill Co., 1967.

[20]Kahaner, D., Moler, C., and Nash, S., *Numerical Methods and Software*, Prentice-Hall, NJ, USA, 1989.

[21]Stoer, J. and Bulirsch, R., *Introduction to Numerical Analysis*, Springer-Verlag, 2002.

[22]Seckel, E. and Curtiss, H. C., "Aerodynamic Characteristics of Helicopter Rotors," Tech. Rep. No. 659, Department of Aerospace and Mechanical Engineering, Princeton University, 1962.

[23]Chen, R., "A Simplified Rotor System Mathematical Model for Piloted Flight Dynamics Simulation," Tech. Rep. NTM 78575, NASA Ames Research Center, 1979.

[24]Gessow, A. and Myers, G., *Aerodynamics of the Helicopter*, College Park Pr, 1999.

[25]Shevell, R., *Fundamentals of Flight*, Prentice Hall, Upper Saddle River NJ, 1989.

[26]Anderson, J., *Fundamentals of Aerodynamics. Third Ed.*, McGraw-Hill Higher Education, NY, 2001.

[27]Zhao, X. and Curtiss, H., "A Study of helicopter Stability and Control Including Blade Dynamics," Tech. Rep. TR 1823T, NASA Ames Research Center, 1988.

[28]Hong, S. and Curtiss, H., "An Analytic Modeling and System Identification Study of Rotor Fuselage Dynamics at Hover," Tech. Rep. CR-192303, NASA, 1993.

[29]Taamallah, S., "A Flight Dynamics Helicopter UAV Model For A Single Pitch-Lag-Flap Main Rotor: Modeling & Simulations," Tech. Rep. NLR-TP-2011-286-PT-1, NLR, 2011.

[30]Leishman, G., *Principles of Helicopter Aerodynamics*, Cambridge University Press, Cambridge, UK, 2000.

[31]Takahashi, M., "A Flight-Dynamic Helicopter Mathematical Model with a Single Flap-Lag-Torsion Main Rotor," Tech. Rep. TM 102267, NASA Ames Research Center, 1990.

[32]Mettler, B., *Identification Modelling and Characteristics of Miniature Rotorcraft*, Kluwer Academic Publishers, Norwell Mass, USA, 2003.

[33]ART, *FLIGHTLAB Theory Manual (Vol. One & Two)*, Advanced Rotorcraft Technology, Inc., Mountain View CA, 2006.

[34]MathWorks, http://www.mathworks.com/, Natick MA., U.S.A.

[35]ART, http://www.flightlab.com/, Mountain View CA., U.S.A.